

Fig. 2—Effect of manganese on the transformation pressures of iron.

tion back to bcc as the pressure is reduced is evidenced by the low intensity of the 1 and 3 lines at 0 kbar. These diffraction patterns clearly demonstrate: a) the bcc \rightleftharpoons hcp nature of the transformation, b) the gradual increase in the amount of the hcp phase as pressure is increased, and c) the transformation of most of the hcp back to bcc as pressure was released.

In the case of the Fe-17.7 pct Mn sample, this basic transformation pattern exhibits some interesting variations. This sample initially has a structure which is about 50 pct fcc and 50 pct hcp in the annealed condition. The diffraction pattern in Fig. 4 (Fe-17.7 pct Mn alloy) taken at 18 kbar nominal pressure (33 kbar actual pressure) shows this untransformed crystallographic structure. The data show that the transformation starts at 26 kbar actual pressure. In Fig. 4, the increase in the intensity of the number three line (1.92Å-hcp) at 30 kbar nominal pressure (47.5 kbar actual pressure) indicates that the transformation then proceeds as pressure is increased until the sample is 100 pct hcp at 50 kbar nominal (120 kbar actual). Upon release of pressure, the hcp structure is retained. Since the sample contains no bcc prior to the beginning of transformation, the transformation which occurs is either a $\gamma \rightarrow \epsilon$ transformation or is due to a $\gamma \rightarrow (\alpha) \rightarrow \epsilon$ type transformation where the fcc first shears to bcc. This bcc then transforms immediately to hcp because the bcc is unstable at this pressure. The necessary $\gamma \rightarrow \alpha \rightarrow \epsilon$ martensitic transformation associated with deformation has been proposed for stainless steels²¹⁻²² and Schumann¹⁹ has observed both a $\gamma \rightarrow \alpha$ and $\gamma \rightarrow \epsilon$ martensitic transformation in Fe-Mn alloys containing 0 to 10, and 14.5 to 27 pct manganese, respectively.

As in the case of pure iron,¹⁰ the transformations for the Fe-Mn alloys are "abaric," i.e., the extent of completion of the transformation is determined by the difference between the applied pressure and the pressure necessary to initiate the transformation. Also,

there is a hysteresis between the pressures required to initiate the forward and reverse transformations. These observations again indicate that the transformation may be of the martensitic type.

Plotted in Fig. 2 is a P_0 curve, or the equilibrium $\alpha \rightleftharpoons \epsilon$ transformation line, determined from the following equation:¹⁰

$$P_0 = \frac{P_{M_s}^{\alpha \rightarrow \epsilon} + P_{M_s}^{\epsilon \rightarrow \alpha}}{2} \quad [1]$$

This equation is the analogue of the Kaufman and Cohen²⁴ equilibrium temperature equation, T_0 , derived for the martensite transformation. Also shown in Fig. 2 is the calculated P_0 line for Fe-Mn alloys.²⁹ This line was determined from the free energy equation:

$$\Delta F^{\alpha \rightarrow \epsilon} [T_1 P_1 x] = (1-x) \Delta F_{Fe}^{\alpha \rightarrow \epsilon} + x \Delta F_{Mn}^{\alpha \rightarrow \epsilon} + x(1-x)(E-A)_{FeMn} + 23.9 P \Delta V^{\alpha \rightarrow \epsilon} \quad [2]$$

where x = atomic fraction Mn

at 300°K $\Delta F_{Fe}^{\alpha \rightarrow \epsilon} = +1010$ cal per g-atom

$\Delta F_{Mn}^{\alpha \rightarrow \epsilon} = +1080$ cal per g-atom

interaction parameter $(E - A)$

$= -6990$ cal per g-atom

$\Delta V^{\alpha \rightarrow \epsilon} = -0.38$ cu cm per g-atom

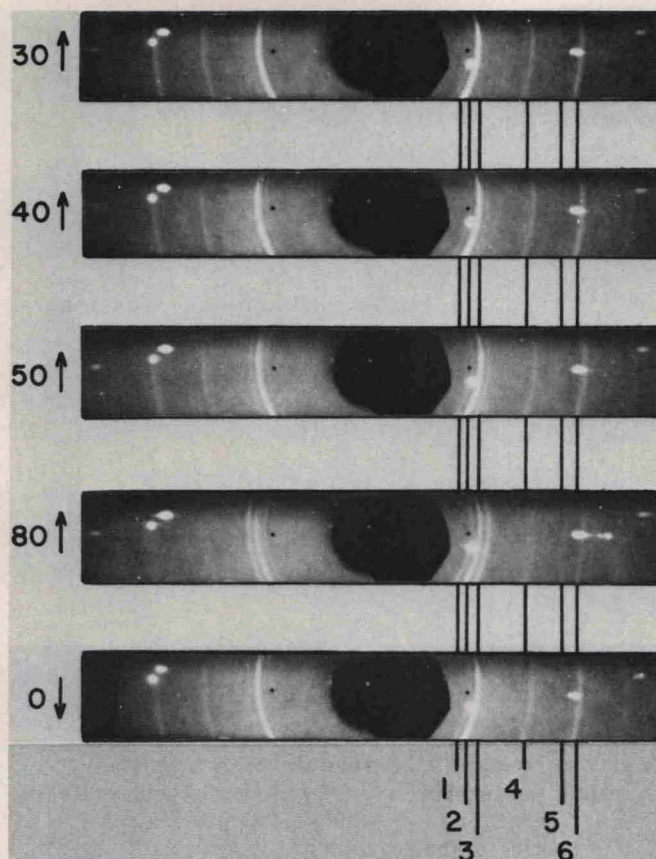
Substituting in Eq. [2]:

$$\Delta F^{\alpha \rightarrow \epsilon} [300, P_0, x] = 0 = (1-x)1010 + x(1080) + x(1-x)(-6990) - 9.082 P_0 \quad [3]$$

or,

$$P_0 \approx 111.2 - 763x + 769x^2 \quad [4]$$

It can be seen that there is substantial agreement be-



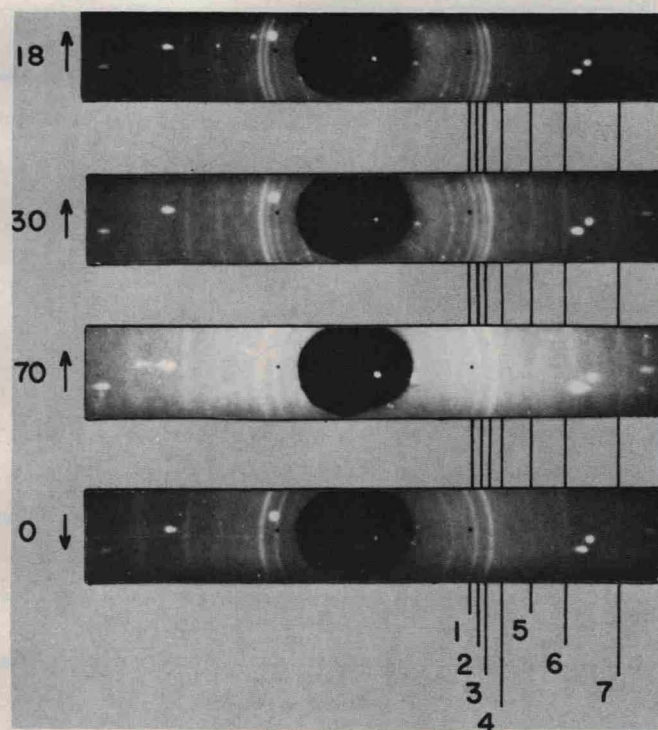
Line	Interplanar Spacing, Å	Phase and Indices
1	2.17	$\epsilon(100)$
2	2.04	$\alpha(110)$ $\epsilon(002)$ $\gamma(111)$
3	1.92	$\epsilon(101)$
4	1.43	$\alpha(200)$
5	1.25	$\epsilon(110)$ $\gamma(220)$
6	1.17	$\alpha(211)$

Fig. 3—High-pressure X-ray diffraction patterns with diffraction lines identified. Sample was iron-4.9 pct manganese. Nominal pressures are given to the left of each diffraction pattern. Arrows pointing up show increasing pressure and arrows pointing down show decreasing pressures.

tween the calculated and the experimentally determined P_0 . Furthermore, the driving force for the bcc \rightarrow hcp martensite transformation, calculated by multiplying the difference in pressure between $P_{M_s}^{\alpha \rightarrow \epsilon}$ and P_0 by $23.9\Delta V$, ranges from 227 cal per g-atom at 0 pct Mn¹⁰ to 150 cal per g-atom at 13.9 pct Mn. This is in good agreement with determined values of 150 to 300 cal per g-atom calculated for the martensite transformation in iron alloys.²⁴

Iron-Nickel-Chromium

The compositions of the Fe-Ni-Cr alloys studied (Table I, series 2A to 2D) were chosen to correspond closely to the composition of alloys which Minshall, Zukas, and Fowler^{11,30} found to have low transformation pressures. Their transformation pressures were determined by means of dynamic pressurization and could not determine the structure of the phase formed at high pressure or the pressure at which it began to return to the ambient-pressure phase during pressure



Line	Interplanar Spacing, Å	Phase and Indices
1	2.17	$\epsilon(100)$
2	2.04	$\alpha(110)$ $\epsilon(002)$ $\gamma(111)$
3	1.92	$\epsilon(101)$
4	1.79	$\gamma(200)$
5	1.48	$\epsilon(102)$
6	1.25	$\epsilon(110)$ $\gamma(220)$
7	1.08	$\epsilon(112)$ $\gamma(311)$

Fig. 4—High-pressure X-ray diffraction patterns with diffraction lines identified. Sample was iron-17.7 pct manganese. Nominal pressures are given to the left of each diffraction pattern. Arrows pointing up show increasing pressure and arrows pointing down show decreasing pressure.

release. Also, the alloy compositions selected are close to those of some grades of stainless steels. The transformations in these materials are of considerable commercial importance, and several papers are available that deal with the transformations in such alloys under conditions of varying thermomechanical processes.^{21-23,25-27}

Table III shows the percentage of phases present for these alloys at 0, 25, and 155 kbar as pressure was increased and at ambient pressure after all pressure was released. It can be seen that γ as well as α and ϵ phases are present in these alloys and that the transformations begin at much lower pressures than were observed in the Fe-Mn alloys. It is also evident that the 11.6 pct Ni-17.4 pct Cr alloy and the 12.3 pct Ni-13.5 pct Cr alloy retain their high pressure structure after pressure is released. This demonstrates that combined nickel and chromium additions promote the formation and stability of the hcp phase.

In Fig. 5, the combined alloying effects of Ni + Cr on the $\alpha \rightarrow \epsilon$ martensitic transformation of iron are plotted using the results of this investigation as well as the data of Fowler *et al.*^{11,30} and Gust and Royce.¹⁵ A smooth curve has been drawn through the data from